Nuclear shadowing in deep-inelastic scattering on nuclei: Comparing predictions of three unitarization schemes

F. Carvalho,[1] V. P. Gonçalves,[2] F. S. Navarra,[3] and E. G. de Oliveira[3]

[1]*Departamento de Ciências Exatas e da Terra, Universidade Federal de São Paulo, Campus Diadema, Rua Professor Artur Riedel, 275 Jd. Eldorado, 09972-270 Diadema, São Paulo, Brazil*

[2]*High and Medium Energy Group (GAME), Instituto de Física e Matemática, Universidade Federal de Pelotas, Caixa Postal 354, 96010-900 Pelotas, Rio Grande do Sul, Brazil*

[3]*Instituto de Física, Universidade de São Paulo, Caixa Postal 66318, 05315-970 São Paulo, São Paulo, Brazil*

(Received 30 September 2012; revised manuscript received 2 April 2013; published 20 June 2013)

The measurement of the nuclear structure functions $F_2^A(x, Q^2)$ and $F_L^A(x, Q^2)$ at the future electron-ion collider will be of great relevance to understanding the origin of nuclear shadowing and to probe gluon saturation effects. Currently there are several phenomenological models, based on very distinct approaches, which describe the scarce experimental data quite successfully. One of main uncertainties comes from the schemes used to include the effects associated with the multiple scatterings and to unitarize the cross section. In this paper we compare the predictions of three distinct unitarization schemes of the nuclear structure function F_2^A that use the same theoretical input to describe the projectile-nucleon interaction. In particular, we consider as input the predictions of the color glass condensate formalism, which reproduce the inclusive and diffractive *ep* HERA data. Our results demonstrate that experimental analysis of F_2^A is able to discriminate between the unitarization schemes.

DOI: 10.1103/PhysRevC.87.065205 PACS number(s): 24.85.+p, 13.60.−r

I. INTRODUCTION

The measurement of the nuclear structure function in deep-inelastic electron-nucleus scattering (DIS) is the best way to improve our knowledge of the nuclear parton distributions and QCD dynamics in a high energy regime (see, e.g., Refs. [1,2]). However, after more than 30 years of experimental and theoretical studies, a standard picture of nuclear modifications of structure functions and parton densities has not yet emerged. Fixed-target DIS measurement on nuclei has revealed that the ratio of nuclear to nucleon structure functions (normalized by the atomic mass number) is significantly different from unity. In particular, these data demonstrate an intricate behavior, with the ratio being less than 1 at large x (the EMC effect) and at small x (shadowing) and larger than 1 for $x \approx 10^{-1}$ (antishadowing). The existing data were taken at lower energies [3] and therefore the perturbative QCD regime ($Q^2 \geqslant 1$ GeV^2) was explored only for relatively large values of the (Bjorken) x variable ($x > 10^{-2}$). Experimentally, this situation will hopefully change with a future high-energy electron-ion collider (EIC) (For recent reviews see, e.g., Refs. [4,5]), which is supposed to take data at higher energies and explore the region of small x in the perturbative QCD regime. In the case of the Large electron Hadron Collider (LeHC), it will be possible to reach values as low as $x = 10^{-5}$.

The theory of nuclear effects in DIS is still far from being concluded. The straightforward use of nucleon parton distributions evolved with Dokshitzer-Gribov-Lipatov-Altarelli-Parisi (DGLAP) equations and corrected with a nuclear modification factor determined by fitting the existing data as in Refs. [6–11] is well justified only in the large Q^2 region and with not too small x. Moreover, these approaches do not address the fundamental problem of the origin of the nuclear shadowing and cannot be extended to small x, where we expect to see new interesting physics related to the nonlinear aspects of QCD and gluon saturation (for reviews, see Ref. [12]). Currently, there are several phenomenological models that predict different magnitudes for the shadowing in the nuclear structure function based on distinct treatments for the multiple scatterings of the partonic component of the virtual photon, assumed in general to be a quark-antiquark ($q\bar{q}$) color dipole. Some works [13–16] address the origin of the nuclear shadowing through the Glauber-Gribov formalism [17,18] in the totally coherent limit ($l_c \approx 1/2m_N x \gg R_A$, where l_c is coherence length), which considers the multiple scattering of the color dipole with a nucleus made of nucleons whose binding energy is neglected. In the high-energy limit, the eikonal approximation is assumed, with the dipole keeping a fixed size during the scattering process. In this approach the nuclear structure function is given by

$$F_2^A(x, Q^2) = \frac{Q^2}{4\pi^2\alpha_{em}}\left(\sigma_{\gamma^* A}^T + \sigma_{\gamma^* A}^L\right), \tag{1}$$

where the transverse and longitudinal photon-nucleus cross sections are given by

$$\sigma_{\gamma^* A}^{T,L} = \int d^2r \int dz |\psi_{T,L}(r, z)|^2 \sigma_{dA}(x, r). \tag{2}$$

In the above expression $|\psi_{T,L}(r, z)|^2$ is the probability of the transverse (T) or longitudinal (L) photon to split into a $q\bar{q}$ pair of size r and $\sigma_{dA}(x, r)$ is the dipole-nucleus cross section, which is expressed as [13]

$$\sigma_{dA}(x, r) = \int d^2b 2 \left\{1 - \exp\left[-\frac{1}{2} A\, T_A(b) \sigma_{dp}(x, r)\right]\right\}, \tag{3}$$

with $T_A(b)$ being the nuclear thickness function and $\sigma_{dp}(x, r)$ being the dipole-proton cross section. It must be stressed that once $\sigma_{dp}(x, r)$ is fixed, the extension to the nuclear case is essentially parameter free in this approach. In the Glauber formula (3) it is assumed that the dipole undergoes several

elastic scatterings on the target. Although reasonable and phenomenologically successful this assumption deserves further investigation. This model can be derived in the classical approach of the color glass condensate (CGC) formalism [19].

Another approach largely used in the literature is based on the connection between nuclear shadowing and the cross section for the diffractive dissociation of the projectile [20–23], which was established a long time ago by Gribov [18]. Its result can be derived using reggeon calculus [24] and the Abramovsky-Gribov-Kancheli cutting rules [25] and is a manifestation of the unitarity. This formalism can be used to calculate directly cross sections of photon-nucleus scattering for the interaction with two nucleons in terms of the diffractive photon-nucleon cross section. In this formalism, the total photon-nucleus cross section is expressed as a series containing the contribution from multiple scatterings (1, 2, ...),

$$\sigma_{\gamma^* A} = \sigma^{(1)}_{\gamma^* A} + \sigma^{(2)}_{\gamma^* A} + \sigma^{(3)}_{\gamma^* A} + \cdots, \tag{4}$$

with the first term being the one that arises from independent scattering of the photon off A nucleons:

$$\sigma^{(1)}_{\gamma^* A} = A\, \sigma_{\gamma^* p}, \tag{5}$$

and the first correction to the nonadditivity of cross sections being

$$\sigma^{(2)}_{\gamma^* A} = -4\pi A(A-1) \int d^2b\, T_A^2(b) \int_{M^2_{\rm min}}^{M^2_{\rm max}} dM^2 \left.\frac{d\sigma^{\mathcal{D}}_{\gamma^* \rm p}}{dM^2 dt}\right|_{t=0} F_A^2(t_{\rm min}), \tag{6}$$

where M^2 is the mass of the diffractively produced system, F_A is the nucleus form factor which takes into account the coherence effects, and the differential $\gamma^* p$ cross section for the diffractive dissociation of the virtual photon appearing in Eq. (6) is given by

$$\left.\frac{d\sigma^{\mathcal{D}}_{\gamma^* \rm p}(Q^2, x_{I\!P}, \beta)}{dM^2 dt}\right|_{t=0} = \frac{4\pi^2 \alpha_{em} B_D}{Q^2(Q^2+M^2)} x_{I\!P} F^{(3)}_{2\mathcal{D}}(Q^2, x_{I\!P}, \beta), \tag{7}$$

where B_D is the diffractive slope parameter and $x_{I\!P} F^{(3)}_{2\mathcal{D}}(Q^2, x_{I\!P}, \beta)$ is the diffractive proton structure function. Moreover, $t_{\rm min} = -m_N^2 x_{I\!P}^2$, $x_{I\!P} = x/\beta$, and $\beta = Q^2/(Q^2+M^2)$. The integration limits in M^2 are $M^2_{\rm min} = 4m_\pi^2 = 0.08$ GeV^2, $M^2_{\rm max} = Q^2\,(x_{I\!P\rm max}/x - 1)$, and $x_{I\!P\rm max} = 0.1$. A shortcoming of this approach is that the inclusion of the higher-order rescatterings is model dependent. This resummation is especially important at small x, where multiple scattering is more likely to happen. In general it is assumed that the intermediate states in the rescatterings have the same structure and two resummation schemes are considered: (a) *the Schwimmer equation* [26], which sums all fan diagrams with triple pomeron interactions, is valid for the scattering of a small projectile on a large target, and implies that the photon-nucleus cross section is given by

$$\sigma^S_{\gamma^* A}(x,r) = \sigma_{\gamma^* p}(x,r)\, A \int d^2b \frac{T_A(b)}{1 + (A-1)\, T_A(b)\, f(x,Q^2)}, \tag{8}$$

and (b) *the eikonal unitarized cross section*, given by

$$\sigma^E_{\gamma^* A}(x,r) = \sigma_{\gamma^* p}(x,r)\, A \int d^2b \times \frac{\{1 - \exp\left[-2(A-1) T_A(b) f(x,Q^2)\right]\}}{2(A-1) f(x,Q^2)}, \tag{9}$$

where

$$f(x,Q^2) = \frac{4\pi}{\sigma_{\gamma^* p}(x,r)} \times \int_{M^2_{\rm min}}^{M^2_{\rm max}} dM^2 \left.\frac{d\sigma^{\mathcal{D}}}{dM^2 dt}\right|_{t=0} \times F_A^2(t_{\rm min}). \tag{10}$$

As shown in Refs. [22,23], the eikonal unitarization predicts a larger magnitude for the nuclear shadowing than the Schwimmer equation. For models that take into account the possibility of different intermediate states, see, e.g., Ref. [27]. Except for the choice of the resummation scheme, the predictions for $\sigma_{\gamma^* A}$ obtained using Eq. (8) or Eq. (9) are parameter free once the diffractive cross section is provided. Models based on this nonperturbative Regge-Gribov framework are quite successful in describing existing data on inclusive and diffractive ep and eA scattering [23,28]. However, they lack solid theoretical foundations within QCD. It is important to emphasize that some authors [21] use these models as initial conditions for DGLAP evolution.

The comparison among the predictions of the different models for nuclear shadowing presented in Ref. [1], including the models discussed above, shows that they coincide within $\approx$15% in the region where experimental data exist ($x \geqslant 10^{-2}$) but differ strongly for smaller values of x, with the difference being almost of a factor 2 at $x = 10^{-5}$. Our goal in this paper is try to reduce the theoretical uncertainty present in these predictions. In particular, differently from previous studies, which consider different inputs in the calculations using the Glauber, Schwimmer, and eikonal approaches, we consider a unique model for the projectile-nucleon interaction. We calculate the dipole-nucleon cross section and the diffractive structure function using the dipole picture and the solution of the running coupling Balitsky-Kovchegov (BK) equation [29], which is the basic equation of the CGC formalism. Recently, this approach was shown to describe quite well the ep HERA data for inclusive and diffractive observables (see, e.g. Refs. [30–33]). Following this procedure we are able to estimate the magnitude of the theoretical uncertainty associated with the way the multiple scatterings are considered, reducing the contribution associated with the choice of initial conditions used in the calculations. Moreover, we discuss the possibility of discriminating between these unitarization procedures in a future EIC.

This paper is organized as follows. In Sec. II we present a brief description of inclusive and diffrative γ-nucleon processes in the color dipole picture with particular emphasis on the dipole-proton cross section given by the CGC formalism. In Sec. III we present the predictions of the three unitarization schemes discussed above using as input the CGC results for the dipole-proton interaction and compare them with the existing experimental data. Moreover, we present a comparison between the predictions for the kinematical region

which will be probed in a future EIC. Finally, in Sec. IV we summarize our results and present our conclusions.

II. INCLUSIVE AND DIFFRACTIVE γp PROCESSES IN THE COLOR DIPOLE PICTURE

The photon-hadron interaction at high energy (small x) is usually described in the infinite momentum frame of the hadron in terms of the scattering of the photon off a sea quark, which is typically emitted by the small-x gluons in the proton. However, as already mentioned in the Introduction, to describe inclusive and diffractive interactions and disentangle the small-x dynamics of the hadron wave function, it is more adequate to consider the photon-hadron scattering in the dipole frame, in which most of the energy is carried by the hadron, while the photon has just enough energy to dissociate into a quark-antiquark pair before the scattering. In this representation the probing projectile fluctuates into a quark-antiquark pair (a dipole) with transverse separation $\boldsymbol{r}$ long before the interaction, which then scatters off the target [34]. The main motivation to use this color dipole approach is that it gives a simple unified picture of inclusive and diffractive processes. In particular, in this approach the proton structure function is given in terms of the dipole-proton cross section, $\sigma_{dp}(x, r)$, as follows:

$$F_2^p(x, Q^2) = \frac{Q^2}{4\pi^2\alpha_{em}} \int d^2r \int dz |\psi(r, z)|^2 \sigma_{dp}(x, r), \quad (11)$$

where $|\psi(r, z)|^2$ is the probability of the photon to split into a $q\bar{q}$ pair of size r. Moreover, the total diffractive cross sections take the following form (see, e.g., Ref. [35]),

$$\sigma_{T,L}^{\mathcal{D}} = \int_{-\infty}^{0} dt\, e^{B_D t} \frac{d\sigma_{T,L}^{\mathcal{D}}}{dt}\bigg|_{t=0} = \frac{1}{B_D} \frac{d\sigma_{T,L}^{\mathcal{D}}}{dt}\bigg|_{t=0}, \quad (12)$$

where

$$\frac{d\sigma_{T,L}^{\mathcal{D}}}{dt}\bigg|_{t=0} = \frac{1}{16\pi} \int d^2\mathbf{r} \int_0^1 d\alpha |\Psi_{T,L}(\alpha, \mathbf{r})|^2 \sigma_{dp}^2(x, \boldsymbol{r}). \quad (13)$$

It is assumed that the dependence on the momentum transfer, t, factorizes and is given by an exponential with a diffractive slope, B_D. The diffractive processes can be analyzed in more detail by studying the behavior of the diffractive structure function $F_2^{\mathcal{D}(3)}(Q^2, \beta, x_{IP})$. Following Ref. [35] we assume that the diffractive structure function is given by

$$F_2^{\mathcal{D}(3)}(Q^2, \beta, x_{IP}) = F_{q\bar{q},L}^{\mathcal{D}} + F_{q\bar{q},T}^{\mathcal{D}} + F_{q\bar{q}g,T}^{\mathcal{D}}, \quad (14)$$

where the $q\bar{q}g$ contribution with longitudinal polarization is not present because it has no leading logarithm in Q^2. The different contributions can be calculated and for the $q\bar{q}$ contributions they read [36,37]

$$x_{IP} F_{q\bar{q},L}^{\mathcal{D}}(Q^2, \beta, x_{IP}) = \frac{3Q^6}{32\pi^4\beta B_D} \sum_f e_f^2 2 \int_{\alpha_0}^{1/2} d\alpha \alpha^3 (1-\alpha)^3 \Phi_0, \quad (15)$$

$$x_{IP} F_{q\bar{q},T}^{\mathcal{D}}(Q^2, \beta, x_{IP}) = \frac{3Q^4}{128\pi^4\beta B_D} \sum_f e_f^2 2 \int_{\alpha_0}^{1/2} d\alpha \alpha (1-\alpha) \times \left\{\epsilon^2[\alpha^2 + (1-\alpha)^2]\Phi_1 + m_f^2 \Phi_0\right\}, \quad (16)$$

where the lower limit of the integral over α is given by $\alpha_0 = \frac{1}{2}\left(1 - \sqrt{1 - \frac{4m_f^2}{M^2}}\right)$, the sum is performed over the quark flavors, and [38]

$$\Phi_{0,1} \equiv \left[\int_0^\infty r dr K_{0,1}(\epsilon r) \sigma_{dp}(x_{IP}, \boldsymbol{r}) J_{0,1}(kr)\right]^2. \quad (17)$$

The $q\bar{q}g$ contribution, within the dipole picture at leading $\ln Q^2$ accuracy, is given by [35–37]

$$x_{IP} F_{q\bar{q}g,T}^{\mathcal{D}}(Q^2, \beta, x_{IP}) = \frac{81\beta\alpha_S}{512\pi^5 B_D} \sum_f e_f^2 \int_\beta^1 \frac{dz}{(1-z)^3} \left[\left(1 - \frac{\beta}{z}\right)^2 + \left(\frac{\beta}{z}\right)^2\right] \int_0^{(1-z)Q^2} dk_t^2 \ln\left(\frac{(1-z)Q^2}{k_t^2}\right) \times \left[\int_0^\infty u du\, \sigma_{dp}(u/k_t, x_{IP}) K_2\left(\sqrt{\frac{z}{1-z}} u^2\right) J_2(u)\right]^2. \quad (18)$$

As pointed out in Ref. [39], at small β and low Q^2, the leading $\ln(1/\beta)$ terms should be resummed and the above expression should be modified. However, because a description with the same quality using Eq. (18) is possible by adjusting the coupling [39], in what follows we use this expression for our phenomenological studies. We use the standard notation for the variables $x_{IP} = (M^2 + Q^2)/(W^2 + Q^2)$ and $x = Q^2/(W^2 + Q^2) = \beta x_{IP}$, where W the total energy of the $\gamma^* p$ system.

The main input for the calculations of inclusive and diffractive observables in the dipole picture is $\sigma_{dp}(x, \boldsymbol{r})$ which is determined by the QCD dynamics at small x. In the eikonal approximation, it is given by

$$\sigma_{dp}(x, \boldsymbol{r}) = 2 \int d^2\boldsymbol{b}\, \mathcal{N}(x, \boldsymbol{r}, \boldsymbol{b}), \quad (19)$$

where $\mathcal{N}(x, \boldsymbol{r}, \boldsymbol{b})$ is the forward scattering amplitude for a dipole with size $r = |\boldsymbol{r}|$ and impact parameter $\boldsymbol{b}$, which can be related to the expectation value of a Wilson loop [12]. It encodes all the information about the hadronic scattering and thus about the nonlinear and quantum effects in the hadron wave function. In general, it is assumed that the impact parameter dependence of $\mathcal{N}$ can be factorized as $\mathcal{N}(x, \boldsymbol{r}, \boldsymbol{b}) =$

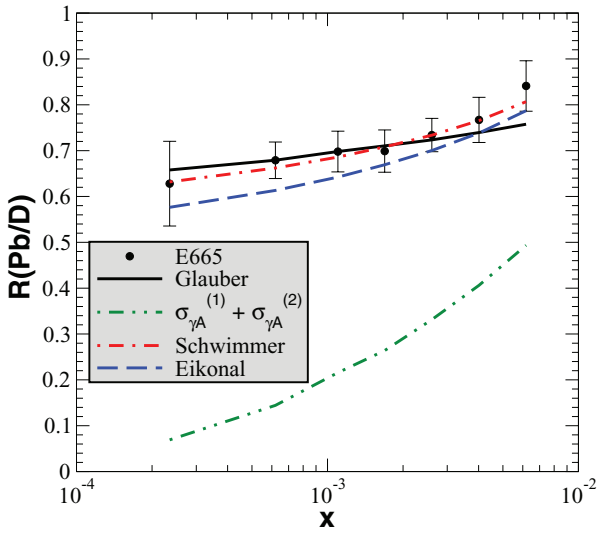

FIG. 1. (Color online) Comparison between the predictions of the distinct models and the E665 experimental data at small x.

$\mathcal{N}(x, \boldsymbol{r})S(\boldsymbol{b})$, where $S(\boldsymbol{b})$ is the profile function in impact parameter space, which implies $\sigma_{dp}(x, \boldsymbol{r}) = \sigma_0 \mathcal{N}(x, \boldsymbol{r})$. The forward scattering amplitude $\mathcal{N}(x, \boldsymbol{r})$ can be obtained by solving the BK evolution equation [30] or considering phenomenological QCD inspired models to describe the interaction of the dipole with the target. BK equation is the simplest nonlinear evolution equation for the dipole-hadron scattering amplitude, being actually a mean field version of the first equation of the B-JIMWLK hierarchy [40]. In its linear version, it corresponds to the Balitsky-Fadin-Kuraev-Lipatov (BFKL) equation [41]. The solution of the leading-order BK equation implies that the saturation scale grows much faster with increasing energy ($Q_s^2 \sim x^{-\lambda}$, with $\lambda \approx 0.5$) than that extracted from phenomenology ($\lambda \sim 0.2 - 0.3$).

In the last years the next-to-leading-order corrections to the BK equation were calculated [42–44] through the ressumation of $\alpha_s N_f$ contributions to all orders, where N_f is the number of flavors. Thanks to these works it is now possible to estimate the soft gluon emission and running coupling corrections to the evolution kernel. The authors have found out that the dominant contributions come from the running coupling corrections, which allow us to determine the scale of the running coupling in the kernel. The solution of the improved BK equation was studied in detail in Ref. [43]. The running of the coupling reduces the speed of the evolution to values compatible with experimental data, with the geometric scaling regime being reached only at ultrahigh energies. In Ref. [30] a global analysis of the small-x data for the proton structure function using the improved BK equation was performed (see also Ref. [45]). In contrast to the BK equation at the leading logarithmic $\alpha_s \ln(1/x)$ approximation, which fails to describe the HERA data, the inclusion of running coupling effects in the evolution renders the BK equation compatible with them (see also Refs. [31–33]). In what follows we consider the BK predictions for $\mathcal{N}(x, \boldsymbol{r})$ (from now on called rcBK) obtained using the Golec-Biernat - Wüsthoff (GBW) [30] initial condition.

III. NUMERICAL RESULTS AND DISCUSSION

A. The F_2^A structure function

In what follows we consider two different nuclei, Ca and Pb, and use the deuteron (D) as a reference to calculate the experimentally measured ratios $R_{\mathrm{Ca}/D} \equiv (2/40)F_2^{\mathrm{Ca}}/F_2^D$ and $R_{\mathrm{Pb}/D} \equiv (2/208)F_2^{\mathrm{Pb}}/F_2^D$. We assume that the diffractive slope parameter is $B_D = 6.7\ \mathrm{GeV}^{-2}$ and that the nucleus form factor is given by

$$F_A(t_{\mathrm{min}}) = \int d^2b\ J_0(b\sqrt{-t_{\mathrm{min}}})T_A(b), \tag{20}$$

where the thickness function is given in terms of the nuclear density ρ_A as

$$T_A(b) = \int_{-\infty}^{+\infty} dz \rho_A(\vec{b}, z),$$

with the normalization fixed by $\int d^2b\ T_A(\vec{b}) = 1$.

In Fig. 1 we compare the predictions of the Glauber (solid line), Schwimmer (dot-dashed line), eikonal (dashed line), and double scattering (dot-dot-dashed line) models for the ratios with the E665 experimental data at small x [3]. Although

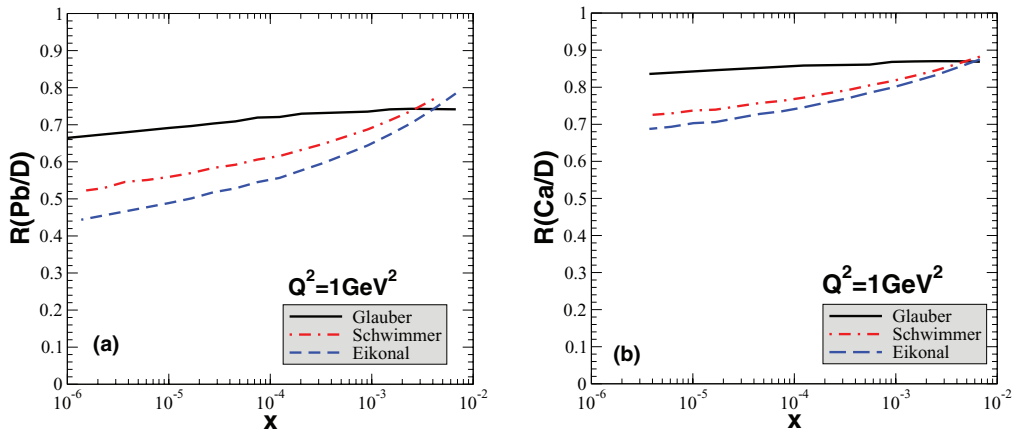

FIG. 2. (Color online) Nuclear ratios as a function of x at $Q^2 = 1\ \mathrm{GeV}^2$. (a) $R_{\mathrm{Pb}/D}$. (b) $R_{\mathrm{Ca}/D}$.

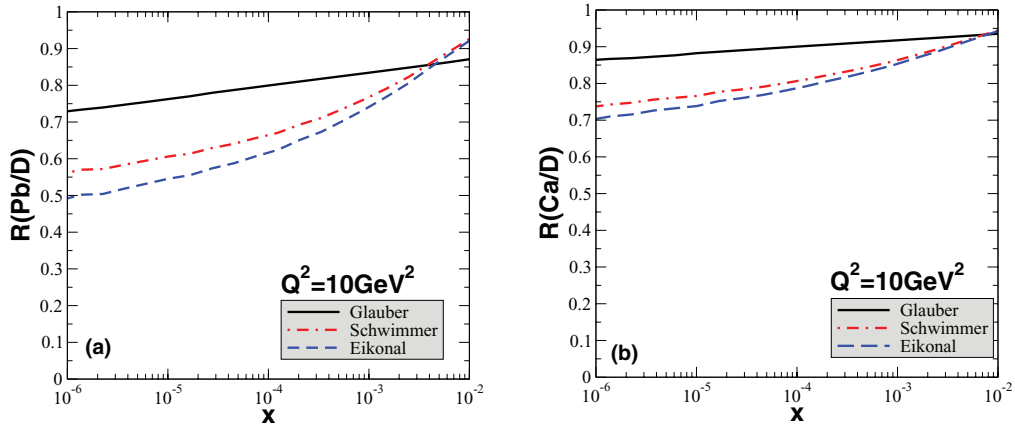

FIG. 3. (Color online) Nuclear ratios as a function of x at $Q^2 = 10$ GeV^2. (a) $R_{\mathrm{Pb}/D}$. (b) $R_{\mathrm{Ca}/D}$.

joined with lines, our results are computed at the same $\langle x \rangle$ and $\langle Q^2 \rangle$ as the experimental data. Our results demonstrate that if we compute the nuclear structure function up to two scatterings, which implies that $\sigma_{\gamma^* A} = \sigma^{(1)}_{\gamma^* A} + \sigma^{(2)}_{\gamma^* A}$, we are not able to describe the experimental data. Furthermore, since the magnitude of the first correction, $\sigma^{(2)}_{\gamma^* A}$, is very large, then there is no hope to estimate the nuclear structure function by just summing a few terms in the multiple scattering series. Therefore, a full resummation of the multiple scatterings is necessary, which makes the predictions model dependent. The agreement with the current experimental data at small x of the Glauber, Schwimmer, and eikonal models is quite reasonable taking into account that no parameters have been fitted to reproduce the data. This implies that the current data are not able to discriminate between the unitarization schemes.

Having in mind that a future EIC is expected to be able to analyze the kinematical region of small x ($x \simeq 10^{-5}$) and $Q^2 \geqslant 1$ GeV^2, we now compute the ratios $R_{\mathrm{Ca}/D}$ and $R_{\mathrm{Pb}/D}$ as a function of x for two different values of Q^2 (=1 and 10 GeV^2). In Fig. 2 we present our predictions for $Q^2 = 1$ GeV^2. It is important to emphasize that in electron scattering the range of x values attainable is kinematically restricted to $x > Q^2/s$, where s is the squared center-of-mass energy, which implies that at $Q^2 = 1$ GeV^2 the smaller values of x in the perturbative region will be probed. At large x ($\approx 10^{-2}$) the predictions almost coincide. However, at small x, the predictions based on the Schwimmer equation or on the eikonal unitarized cross section give a shadowing stronger than that of those based on Glauber-like rescatterings. In particular, at $x \approx 10^{-4}$, the difference between Glauber and Schwimmer is almost 10% in the ratio $R(\mathrm{Ca}/D)$ increasing to $\approx$20% in $R(\mathrm{Pb}/D)$. At this x value, the difference between Schwimmer and eikonal is $\approx$5% and 12% for the ratios $R(\mathrm{Ca}/D)$ and $R(\mathrm{Pb}/D)$, respectively. At smaller values of x, the difference between the three predictions increases, being larger than 20%. Consequently, a measurement of F_2^A at $A = \mathrm{Pb}$ at small x with $\approx$10% precision would be a sensitive test to discriminate between the different models.

In Fig. 3 we present our predictions for the ratios $R_{\mathrm{Ca}/D}$ and $R_{\mathrm{Pb}/D}$ as a function of x at $Q^2 = 10$ GeV^2. The behavior is similar to that observed in Fig. 2. The main point is that the differences between the predictions are not reduced significantly and this makes the discrimination between them possible also at this value of Q^2.

A final comment is in order. The results shown in Figs. 2 and 3 demonstrate that there is a large uncertainty associated with the choice of unitarization scheme used to treat the multiple scatterings and that, in principle, an experimental analysis of the nuclear ratios can be useful to discriminate between these approaches.

Another uncertainty present in the study of the nuclear effects is related to the transition between the linear and nonlinear regimes of the QCD dynamics. We do not know precisely in which kinematical region the predictions obtained using the linear DGLAP evolution cease to be valid. In Fig. 4 we present a comparison of our predictions with those

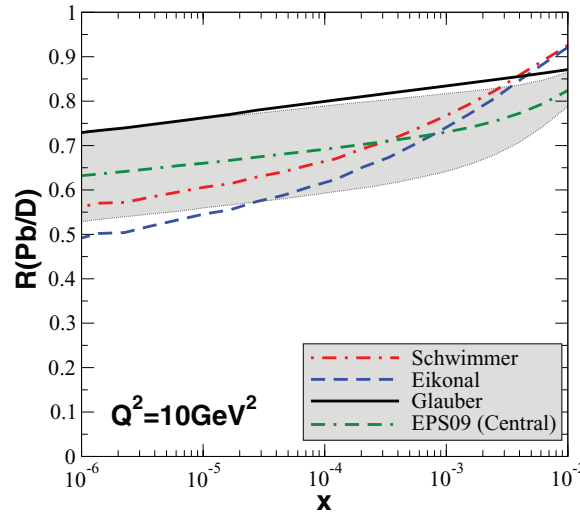

FIG. 4. (Color online) Predictions of the different models discussed in the text. The dash-dash-dot line represents the central value of the prediction obtained with the EPS09 parametrization of the nuclear parton distribution functions. The shaded band represents the theoretical error coming from the uncertainties in the EPS09 parametrization.

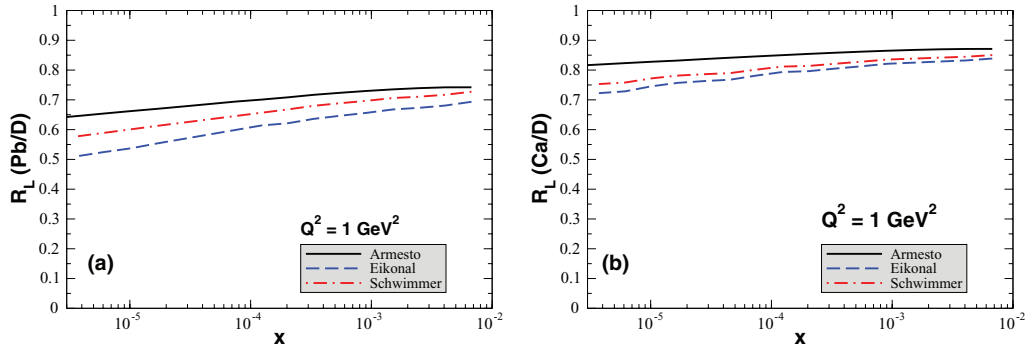

FIG. 5. (Color online) Nuclear ratios as a function of x at $Q^2 = 1$ GeV^2. (a) R_L(Pb/D). (b) R_L(Ca/D).

obtained using the EPS09 [10] parametrization of the nuclear parton distribution functions, which is based on a global fit of the current nuclear data using the DGLAP dynamics. As it can be seen, due to the large theoretical uncertainty in the DGLAP prediction in the small-x region, represented by the shaded band in the figure, it is not possible to draw any firm conclusion about which is the correct framework to describe this observable in future eA colliders. This same conclusion was already obtained in Ref. [14] using a somewhat different approach.

B. The longitudinal structure function

One of the striking features of the proton longitudinal structure function is its strong sensitivity to the gluon distribution. In general, data on F_L are difficult to extract from cross-section measurements, requiring detailed longitudinal-transverse separations in which experiments are performed at the same x and Q^2 but at different energy. As a consequence, the kinematical range spanned by the existing F_L data is rather limited both in the x and the Q^2 coverage. Despite these difficulties F_L has recently been extracted at HERA [46] and also at JLAB (see Ref. [47] for a comprehensive discussion of the data) and its impact on constraining the small-x evolution within the global DGLAP fits is currently under discussion [48]. Measurements of F_L on nuclear targets will be of great importance both for constraining the glue and for studying the nuclear dynamics at small x [49].

In the dipole approach it is straightforward to compute F_L^A and it amounts to using only the longitudinal component of the photon wave function in Eq. (2). In Figs. 5 and 6 we show our results for the ratio $R_L \equiv (2F_L^A)/(AF_L^D)$ for different nuclei. These figures are the analogs of Figs. 2 and 3 for F_L and the comparison between the two sets of figures is instructive. In the figures all the lines follow the expected behavior; i.e., they show that shadowing effects and the corresponding depletion in the nuclear ratios become more pronounced at lower values of x, at lower values of Q^2, and for heavier targets. However, comparing Figs. 2 and 3 with Figs. 5 and 6, we observe that in the latter both target mass number and unitarization scheme dependencies are significantly weaker, which implies the discrimination between the schemes using the F_L^A data is a hard task.

The longitudinal structure function F_L is known to be a very good (better than F_2) probe of the nonlinear effects in the gluon distribution, as shown, for example, in Ref. [50]. Interestingly, our results indicate that the difference between the Glauber, eikonal, and Schwimmer schemes for F_L is smaller than that for F_2. The structure function F_L is thus less sensitive to the different schemes used to unitarize the cross section than F_2. This behavior can be understood as follows. When we treat the multiple scattering problem with the Glauber approach, the only difference between F_2 and F_L comes from the photon wave function in Eq. (2). However, the Eikonal and Schwimmer schemes are strongly dependent on the diffractive ep structure function and this dependence introduces new

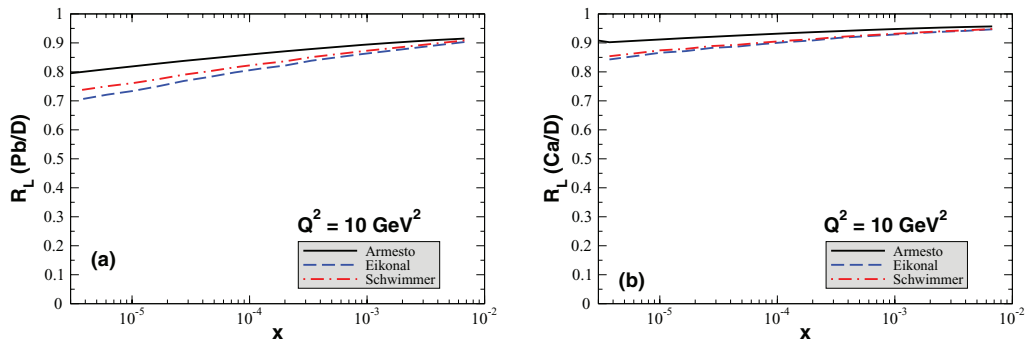

FIG. 6. (Color online) Nuclear ratios as a function of x at $Q^2 = 10$ GeV^2. (a) R_L(Pb/D). (b) R_L(Ca/D).

differences between F_2^A and F_L^A. Whereas in the calculation of F_2^A we include the transverse $q\bar{q}g$ contribution to F_2^D, we do not include this component in the calculation of F_L^A. This leads to the differences observed in the figures.

IV. CONCLUSION

The behavior of the nuclear wave function at high energies provides fundamental information for the determination of the initial conditions in heavy-ion collisions and particle production in collisions involving nuclei. One of the main uncertainties is associated with the magnitude of the nuclear shadowing, which comes mainly from the way in which the multiple scattering problem is treated and from the modeling of the projectile-nucleon interaction. Because a future EIC will probe the shadowing region while keeping sufficiently large Q^2, new studies that determine the main sources of uncertainties in the predictions are necessary. In this work we compare three frequently used approaches to estimate the nuclear shadowing in nuclear DIS. Because in these approaches the nuclear cross section is completely determined once the interaction of the projectile with the nucleon is specified, we considered a single model (rcBK) for input of our calculations to quantify the theoretical uncertainty that comes from the choice of the unitarization model. In particular, we calculate the nuclear ratio between structure functions considering the Glauber, Schwimmer, and eikonal approaches down to very low x utilizing the rcBK results for both inclusive and diffractive cross sections in $\gamma^* p$ scattering. Our results demonstrate that the current experimental data at small x are described successfully by the three approaches. However, the difference between their predictions becomes large in the kinematical region which will be probed in the future EICs. Finally, the study of other observables, such as the nuclear diffractive structure function [51,52] and nuclear vector meson production [16,53], should also be considered to discriminate between the linear and nonlinear regimes. To summarize, to learn more about the unitarization schemes using the nuclear ratios we must disentangle the nonlinear and linear regimes of the QCD dynamics. Our estimates show that due to the large freedom present in the DGLAP analysis they predict similar magnitudes for the nuclear ratios, which implies that a combined analysis of several observables is necessary.

ACKNOWLEDGMENTS

This work was partially financed by the Brazilian funding agencies CAPES, CNPq, and FAPESP.

[1] N. Armesto, J. Phys. G **32**, R367 (2006).
[2] L. Frankfurt, V. Guzey, and M. Strikman, Phys. Rep. **512**, 255 (2012).
[3] M. R. Adams *et al.* (E665 Collaboration), Z. Phys. C **67**, 403 (1995).
[4] D. Boer *et al.*, arXiv:1108.1713.
[5] J. L. Abelleira Fernandez *et al.* (LHeC Study Group Collaboration), J. Phys. G **39**, 075001 (2012).
[6] K. J. Eskola, V. J. Kolhinen, and P. V. Ruuskanen, Nucl. Phys. B **535**, 351 (1998).
[7] K. J. Eskola, V. J. Kolhinen, and C. A. Salgado, Eur. Phys. J. C **9**, 61 (1999).
[8] M. Hirai, S. Kumano, and T. H. Nagai, Phys. Rev. C **76**, 065207 (2007).
[9] D. de Florian and R. Sassot, Phys. Rev. D **69**, 074028 (2004); D. de Florian, R. Sassot, P. Zurita, and M. Stratmann, *ibid.* **85**, 074028 (2012).
[10] K. J. Eskola, H. Paukkunen, and C. A. Salgado, J. High Energy Phys. 04 (2009) 065.
[11] I. Helenius, K. J. Eskola, H. Honkanen, and C. A. Salgado, J. High Energy Phys. 07 (2012) 073.
[12] F. Gelis, E. Iancu, J. Jalilian-Marian, and R. Venugopalan, Annu. Rev. Nucl. Part. Sci. **60**, 463 (2010); E. Iancu and R. Venugopalan, in *Quark Gluon Plasma 3*, edited by R. C. Hwa and X.-N. Wang (World Scientific), p. 106. arXiv:hep-ph/0303204; H. Weigert, Prog. Part. Nucl. Phys. **55**, 461 (2005); J. Jalilian-Marian and Y. V. Kovchegov, *ibid.* **56**, 104 (2006).
[13] N. Armesto, Eur. Phys. J. C **26**, 35 (2002).
[14] E. R. Cazaroto, F. Carvalho, V. P. Goncalves, and F. S. Navarra, Phys. Lett. B **671**, 233 (2009).
[15] V. P. Goncalves, M. S. Kugeratski, and F. S. Navarra, Phys. Rev. C **81**, 065209 (2010).
[16] V. P. Goncalves, M. S. Kugeratski, M. V. T. Machado, and F. S. Navarra, Phys. Rev. C **80**, 025202 (2009); E. R. Cazaroto, F. Carvalho, V. P. Goncalves, M. S. Kugeratski, and F. S. Navarra, Phys. Lett. B **696**, 473 (2011).
[17] R. J. Glauber, in *Lecture in Theoretical Physics*, edited by W. E. Brittin and L. G. Duham (Interscience, New York, 1959), Vol. 1.
[18] V. N. Gribov, Sov. Phys. JETP **29**, 483 (1969); **30**, 709 (1970).
[19] R. Venugopalan, Acta Phys. Polon. B **30**, 3731 (1999).
[20] A. Capella, A. Kaidalov, C. Merino, D. Pertermann and J. Tran Thanh Van, Eur. Phys. J. C **5**, 111 (1998).
[21] L. Frankfurt, V. Guzey, M. McDermott, and M. Strikman, J. High Energy Phys. 02 (2002) 027; L. Frankfurt, V. Guzey, and M. Strikman, Phys. Rev. D **71**, 054001 (2005); Phys. Lett. B **586**, 41 (2004).
[22] N. Armesto, A. Capella, A. B. Kaidalov, J. Lopez-Albacete, and C. A. Salgado, Eur. Phys. J. C **29**, 531 (2003).
[23] N. Armesto, A. B. Kaidalov, C. A. Salgado, and K. Tywoniuk, Eur. Phys. J. C **68**, 447 (2010).
[24] V. N. Gribov, Sov. Phys. JETP **26**, 414 (1968) [Zh. Eksp. Teor. Fiz. **53**, 654 (1967)].
[25] V. A. Abramovsky, V. N. Gribov, and O. V. Kancheli, Yad. Fiz. **18**, 595 (1973) [Sov. J. Nucl. Phys. **18**, 308 (1974)].
[26] A. Schwimmer, Nucl. Phys. B **94**, 445 (1975).
[27] B. Z. Kopeliovich, J. Raufeisen, and A. V. Tarasov, Phys. Lett. B **440**, 151 (1998); Phys. Rev. C **62**, 035204 (2000); J. Nemchik, *ibid.* **68**, 035206 (2003).
[28] N. Armesto, A. B. Kaidalov, C. A. Salgado, and K. Tywoniuk, Phys. Rev. D **81**, 074002 (2010).
[29] I. Balitsky, Nucl. Phys. B **463**, 99 (1996); Y. V. Kovchegov, Phys. Rev. D **60**, 034008 (1999); **61**, 074018 (2000).

[30] J. L. Albacete, N. Armesto, J. G. Milhano, and C. A. Salgado, Phys. Rev. D **80**, 034031 (2009).
[31] M. A. Betemps, V. P. Goncalves, and J. T. de Santana Amaral, Eur. Phys. J. C **66**, 137 (2010).
[32] J. L. Albacete and C. Marquet, Phys. Lett. B **687**, 174 (2010).
[33] V. P. Goncalves, M. V. T. Machado, and A. R. Meneses, Eur. Phys. J. C **68**, 133 (2010).
[34] N. N. Nikolaev and B. G. Zakharov, Z. Phys. C **49**, 607 (1991); **53**, 331 (1992).
[35] K. J. Golec-Biernat and M. Wusthoff, Phys. Rev. D **59**, 014017 (1998); **60**, 114023 (1999).
[36] M. Wusthoff, Phys. Rev. D **56**, 4311 (1997).
[37] N. N. Nikolaev and B. G. Zakharov, J. Exp. Theor. Phys. **78**, 598 (1994); Z. Phys. C **64**, 631 (1994); N. N. Nikolaev, W. Schaefer, B. G. Zakharov, and V. R. Zoller, JETP Lett. **80**, 371 (2004).
[38] J. R. Forshaw, R. Sandapen, and G. Shaw, Phys. Lett. B **594**, 283 (2004).
[39] C. Marquet, Phys. Rev. D **76**, 094017 (2007).
[40] E. Iancu, A. Leonidov, and L. McLerran, Nucl. Phys. A **692**, 583 (2001); E. Ferreiro, E. Iancu, A. Leonidov, and L. McLerran, *ibid.* **703**, 489 (2002); J. Jalilian-Marian, A. Kovner, L. McLerran, and H. Weigert, Phys. Rev. D **55**, 5414 (1997); J. Jalilian-Marian, A. Kovner, A. Leonidov, and H. Weigert, *ibid.* **59**, 014014 (1998); J. Jalilian-Marian, A. Kovner and H. Weigert, *ibid.* **59**, 014015 (1998); J. Jalilian-Marian, A. Kovner, A. Leonidov, and H. Weigert, *ibid.* **59**, 034007 (1999); A. Kovner, J. G. Milhano, and H. Weigert, *ibid.* **62**, 114005 (2000); H. Weigert, Nucl. Phys. A **703**, 823 (2002).
[41] L. N. Lipatov, Sov. J. Nucl. Phys. **23**, 338 (1976) [Yad. Fiz. **23**, 642 (1976)]; E. A. Kuraev, L. N. Lipatov, and V. S. Fadin, Sov. Phys. JETP **45**, 199 (1977) [Zh. Eksp. Teor. Fiz. **72**, 377 (1977)]; I. I. Balitskii and L. N. Lipatov, Sov. J. Nucl. Phys. **28**, 822 (1978).
[42] Y. V. Kovchegov and H. Weigert, Nucl. Phys. A **784**, 188 (2007); **789**, 260 (2007); Y. V. Kovchegov, J. Kuokkanen, K. Rummukainen, and H. Weigert, *ibid.* **823**, 47 (2009).
[43] J. L. Albacete and Y. V. Kovchegov, Phys. Rev. D **75**, 125021 (2007).
[44] I. Balitsky, Phys. Rev. D **75**, 014001 (2007); I. Balitsky and G. A. Chirilli, *ibid.* **77**, 014019 (2008).
[45] J. Kuokkanen, K. Rummukainen, and H. Weigert, Nucl. Phys. A **875**, 29 (2012).
[46] F. Aaron *et al.*, Eur. Phys. J. C **71**, 1579 (2011).
[47] P. Monaghan, A. Accardi, M. E. Christy, C. E. Keppel, W. Melnitchouk, and L. Zhu, arXiv:1209.4542.
[48] N. Armesto, H. Paukkunen, C. A. Salgado, and K. Tywoniuk, Phys. Lett. B **694**, 38 (2010).
[49] M. S. Kugeratski, V. P. Goncalves, and F. S. Navarra, Eur. Phys. J. C **46**, 465 (2006).
[50] E. R. Cazaroto, F. Carvalho, V. P. Goncalves, and F. S. Navarra, Phys. Lett. B **669**, 331 (2008).
[51] M. S. Kugeratski, V. P. Goncalves, and F. S. Navarra, Eur. Phys. J. C **46**, 413 (2006).
[52] H. Kowalski, T. Lappi, and R. Venugopalan, Phys. Rev. Lett. **100**, 022303 (2008); H. Kowalski, T. Lappi, C. Marquet, and R. Venugopalan, Phys. Rev. C **78**, 045201 (2008).
[53] A. Caldwell and H. Kowalski, Phys. Rev. C **81**, 025203 (2010); T. Lappi and H. Mantysaari, *ibid.* **83**, 065202 (2011).